This is a repository copy of *Gain optimization in optically pumped AlGaAs unipolar quantum-well lasers*.

White Rose Research Online URL for this paper:
http://eprints.whiterose.ac.uk/716/

Gain Optimization in Optically Pumped AlGaAs Unipolar Quantum-Well Lasers

Stanko Tomić, Vitomir Milanović, and Zoran Ikonić

Abstract—**A method is described for the optimized design of quantum-well (QW) structures, in respect to maximizing the stimulated gain in optically pumped intersubband lasers. It relies on applying supersymmetric quantum mechanics (SUSYQM) to an initial Hamiltonian, in order to both map one bound state below the spectral range of the initial Hamiltonian, and to generate a parameter-controlled family of isospectral Hamiltonians with the desired energy spectrum. By varying the control parameter, one changes the potential shape and, thus, the values of dipole matrix elements and electron–phonon scattering matrix elements. The use of this procedure is demonstrated by designing smoothly graded and stepwise-constant $Al_xGa_{1-x}As$ ternary alloy QWs, with the self-consistent potential taken into account. Finally, the possibility of employing layer interdiffusion to get optimal smooth potentials is discussed.**

Index Terms—**Layer interdiffusion, quantum-well lasers, supersymmetric quantum mechanics.**

I. INTRODUCTION

SINCE the first proposal of the unipolar semiconductor laser, based on intersubband transitions in quantum wells (QWs) by Kazarinov and Suris in 1971 [1], there has been considerable research effort in this area. This was particularly boosted by the development of molecular beam epitaxy (MBE), which made possible the realization of appropriate structures. Various operating schemes for unipolar lasers have been proposed, and some of them realized, the most important of which is the quantum cascade laser (QCL), demonstrated by Faist *et al.* [2], and realized in the AlInAs–GaInAs alloy system. It is current pumped, and covers the mid-infrared range 4–11 μm [3], [4]. The QCL has recently been realized in the GaAs–AlGaAs alloy, as well [5]. Furthermore, QW lasers comprising InAsSb–InAsSbP superlattices have been made, covering the 3–5 -μm range [6]. Toward the short wavelength range, AlAsSb–InAs based QWLs have been made that take advantage of a large band offset in this system and emit down to 1.9 μm [7]. Lasers based on transitions between the valence subbands, taking advantage of the in-plane effective mass inversion, have been proposed, though not yet realized [8], [9].

In the range of longer wavelengths, the optically pumped intersubband lasers may offer some advantages over the electrically pumped ones, notably the high selectivity of excitation of the relevant states, and freedom from losses due to electron migration toward electrical contacts. In this class, the GaAs–AlGaAs multiple QW (MQW) structures have been considered for far-infrared applications [10], and the asymmetric coupled QWs for the mid-infrared range [11]. Among the optically pumped lasers, we may mention the proposal of tunable (8–12 μm) lasers based on electronic Raman scattering in GaAs–AlGaAs QWs [12], [13].

Among the most important issues in the design of intersubband lasers is the maximization of gain. This may be accomplished via careful tailoring of the QW profile. In the first attempt to maximize the gain of optically pumped QW laser [14] the profile of an asymmetric step QW was varied so as to maximize the square of the dipole matrix elements relevant for the optical pump and for the lasing transition. Gain may be also increased by increasing the carrier density [15]. However, this route leads to an increased equilibrium population of the lower laser state, therefore demanding strong optical pumping to reach threshold. To some extent, this problem may be overcome by optimizing the asymmetric coupled QWs (ACQW), and by increasing the spacing between the ground state and lower laser state, though this drives the electron–phonon relaxation process away from resonance [16]. In further, more advanced design considerations, the influence of interface and confined phonons on electron relaxation times, as well as on carrier heating, for a range of optical pump powers, has also been included [17], [18]. Finally, we note that the optimization of the gain/loss ratio was also considered [19], [20].

Aside from the optical transition matrix elements, for obtaining large inversion (and, hence, gain) it is essential to have fast relaxation of the lower laser level. This proceeds mostly via optical phonons and, to a smaller exten,t via the acoustic phonons. The scattering rate depends on both the levels spacing and the wavefunctions. Furthermore, the spacing between the laser upper and ground states has to be matched to the pump laser wavelength, and this transition has to be allowed, just as is the lasing transition; hence, the structure must be asymmetric, in that the QWs must not be of the same thickness (this applies for a three-level system, as discussed in more detail in Section II-A).

In this paper, we discuss a systematic procedure for optimization the QW profile with respect to maximizing the gain, where the gain dependence not only on the dipole matrix elements, but also on the levels relaxation rates, is accounted for. The procedure relies on supersymmetric quantum mechanics (SUSYQM) [21], [22]. This formalism enables one to manipulate the states of a quantum system (deletion and/or insertion of a state, while leaving others intact) by changing the potential and, at the same time, it introduces one or more free pa-

rameters via which the potential shape may be further varied isospectrally, that is, preserving the states energies ("parameter controlled family of isospectral potentials"). Variation of the potential does affect the wavefunctions, however, in contrast to energies and, therefore, the values of matrix elements involving these states, and eventually the physical property of interest. It remains, therefore, to scan the value of the target function in the space of free parameter(s) and spot the value(s) giving the optimal potential. The resulting optimized potential we derive is realizable by continuous grading of the $Al_xGa_{1-x}As$ alloy, either directly or by using the layer interdiffusion method, starting with a relatively simple stepwise-constant structure with just a few layers. Alternatively, the optimized potential may be discretized, corresponding to a step-graded structure with some reasonable number of layers.

II. THEORETICAL CONSIDERATIONS

A. Stimulated Gain

Consider a three-level intersubband laser, with levels 2 and 3 being the lower and upper laser states, and level 1 the ground state. The modal gain G_m for the stimulated emission is given by [15]

$$G_m = \sigma_{32}\Delta n \qquad (1)$$

where σ_{32} is the lasing transition cross section, and $\Delta n = n_3 - n_2$ is the population inversion (per unit well surface) between states 3 and 2. It has been a rather common practice in the literature to state the values of gain $g = G_m/L_W$, where L_W is the "effective" width of the QW structure, but this may lead to incorrect conclusions when comparing different structures, as discussed, e.g., in [23]. What really matters is the modal gain, and this is the quantity we consider.

Assuming the transition lifetimes between the relevant states known, one may use the rate equations for the three-level system to find the population inversion and the gain. These equations read:

$$\frac{d\delta n_i}{dt} = \frac{S\sigma_{13}}{\hbar\omega_p}(n_1 - n_3)(\delta_{i1} - \delta_{i3})$$
$$+ \sum_{j>i}\frac{\delta n_j}{\tau_{ji}} - \delta n_i \sum_{i>j}\frac{1}{\tau_{ij}} \qquad (2)$$

where $i, j = 1, 2, 3$, $\delta n_i = n_i - \overline{n}_i$, and n_i (or $\overline{n}_i$), in cm^{-2} units, is the actual (or equilibrium) electron density in ith state. Furthermore, S (kW/cm^2) and $\hbar\omega_p$ are the pump laser intensity and photon energy (e.g., $\hbar\omega_p = 116$ meV for the CO_2 laser pump), σ_{13} is the pump absorption cross section, and δ_{ij} is the Kronecker delta symbol. Assuming the conservation of the total number of electrons, in the stationary case ($d/dt \equiv 0$), the system (2) may be solved to find the electron densities in the three states.

For pump powers that are not excessively large, one can set n_2, $n_3 \ll n_1$ and get $n_3 \approx S\sigma_{13}\tau_3 n_1/\hbar\omega_{31}$, where $\tau_3 = (\tau_{31}^{-1} + \tau_{32}^{-1})^{-1}$ is the carriers lifetime in the third subband. This approximation is fully justified in real systems. The simplified

expression for gain then reads [15]

$$G_m \approx \left(1 - \frac{\tau_{21}}{\tau_{32}}\right)\frac{S}{\hbar\omega_p}\sigma_{13}\sigma_{32}\tau_3 n_1$$
$$- \sigma_{32}\frac{m^*k_BT}{\pi\hbar^2}\ln\left[1 + \exp\left(\frac{E_F - E_2}{k_BT}\right)\right] \qquad (3)$$

in which the first term is always (under normal circumstances) dominant over the second one, which accounts for the thermally equilibrium population of the lower laser state. One can now proceed to optimize the gain as given by (3), but the resulting design would then be specific to the operating temperature T and the Fermi level E_F (i.e., the carriers density) chosen. To obtain more generally applicable results, and in view of the fact that the first term in (3) is much more important than the second one, in this work we choose to optimize only the first term. The quantities in it depend on the QW profile (the transition lifetimes τ_{ij} are only weakly dependent on the pump intensity [17], so this may be neglected), and do not depend on T and E_F. Only later, when checking the gain in the final design, will we use the exact expression (1).

Taking the refractive index (for the phase velocity) in the GaAs–AlGaAs alloy to be $\tilde{n} = 3.3$ [15] and the transition line width $\Gamma = 4.25$ meV [17], [24] at $T = 77$ K, the transition cross section is given by $\sigma_{ij}[\text{cm}^2] = 6.533 \times 10^{-19}\Delta E_{ij}[\text{meV}]z_{ij}^2[\text{Å}^2]$. Therefore, the gain in the optically pumped intersubband laser is proportional to the factor

$$\Xi = \left(1 - \frac{\tau_{21}}{\tau_{32}}\right)\tau_3 z_{13}^2 z_{23}^2 \qquad (4)$$

in which only those terms relevant for this work (i.e., which can be varied by suitable tailoring of the QW profile) are retained. Furthermore, the dipole matrix elements in (4) are given by $z_{ij} = \langle i|z|j\rangle$ and the transition lifetime τ_{ij} is the inverse of the total scattering rate: $\tau_{ij} = 1/(W_{ij}^a + W_{ij}^{po})$. The acoustic phonon scattering rate is given by [10]

$$W_{ij}^a = \frac{D_c^2 k_b T m^*}{2\pi c_L\hbar^3}\int|G_{ij}(q_z)|^2\,dq_z \qquad (5)$$

where

D_c conduction band deformation potential;
c_L elastic constant;
k_B Boltzmann's constant;
q_z phonon wavevector in the growth direction.

For bulk-like polar optical phonon scattering, the Frölich interaction is used

$$W_{ij}^{po}(k_{\|})$$
$$= \frac{e^2\omega_{LO}[n(\omega_{LO}) + 1]}{8\pi\epsilon_p}$$
$$\cdot\int\frac{|G_{ij}(q_z)|^2}{\sqrt{\left(\frac{\hbar^2 k_{\|}q_z}{m^*}\right)^2 + \left(\frac{\hbar^2 q_z^2}{2m^*} + E_i - E_j - \hbar\omega_{LO}\right)^2}}\,dq_z$$
$$(6)$$

with $\varepsilon_p = (\varepsilon_s^{-1} - \varepsilon_\infty^{-1})^{-1}$, where $\varepsilon_s = 12.51$ and $\varepsilon_\infty = 10.67$ denote the static and high-frequency permittivities of the AlGaAs alloy [25]. The values of ω_{LO} and ε_p are taken to be constant throughout the structure. The function $G_{ij}(q_z) = \langle i | e^{iq_z z} | j \rangle$ is the electron–phonon interaction overlap integral and $n(\omega_{\mathrm{LO}}) = [\exp(\hbar\omega_{\mathrm{LO}}/k_B T) - 1]^{-1}$ is the Bose–Einstein distribution.

Maximization of the gain [i.e., the term Ξ, in (4)] may thus be accomplished via changing the QW profile which, in turn, changes the wavefunctions and, hence, all the terms on which Ξ depends. It should be noted that in the optically pumped laser, the condition $z_{13} \neq 0$ has to be satisfied (for the pump to be absorbed), implying that the structure has to be asymmetric, i.e., the potential cannot be an even function of space coordinate, i.e., it requires QWs of different thickness. In addition, in order to obtain a population inversion with reasonable effort, the lower laser state should relax much faster than the upper one, which is achieved by choosing the lower laser level to be spaced by the polar optical phonon energy from the ground state ($\hbar\omega_{\mathrm{LO}} = 36$ meV in GaAs [26]). These are the constraints imposed in the variation of the QW profile.

B. SUSYQM Addition of a Bound State

As noted in the Introduction, the variation of the potential is performed via the SUSYQM transform, which will modify the original potential (Hamiltonian) so to have a new bound state added, and also introduce a free parameter into the new Hamiltonian, enabling the potential shape to be varied in an isospectral manner. The description of how this technique is implemented is given next.

The motion of an electron with a constant effective mass m^*, in the potential $U^{(0)}(z)$, is described by the Hamiltonian

$$H^{(0)} = -\frac{\hbar^2}{2m^*}\frac{d^2}{dz^2} + U^{(0)}(z), \qquad (7)$$

with eigenenergies $E_i^{(0)}$ and eigenfunctions $\psi_i^{(0)}$, where $i = 1, 2, \ldots$. This Hamiltonian may be factorized via d'Alambert operators [22]

$$H^{(0)} = AA^\dagger + E_\epsilon \qquad (8)$$

where the factorization state is taken at an energy E_ϵ, below the ground state energy ($E_\epsilon < E_1^{(0)}$), exactly where a new bound state will be subsequently added. The operators A and $A^\dagger$ are mutually adjoint, and have the form

$$A = \frac{\hbar}{\sqrt{2m^*}}\frac{d}{dz} + \mathcal{W}(z), \quad A^\dagger = -\frac{\hbar}{\sqrt{2m^*}}\frac{d}{dz} + \mathcal{W}(z) \quad (9)$$

where $\mathcal{W}(z)$ is the superpotential (the solution of the Ricatti differential equation obtained from $(AA^\dagger + E_\epsilon)\psi_\epsilon^{(0)} = E_\epsilon\psi_\epsilon^{(0)}$) and reads

$$\mathcal{W}(z) = \frac{\hbar}{\sqrt{2m^*}}\frac{d}{dz}\ln\psi_\epsilon^{(0)}(z). \qquad (10)$$

Now we start with the Hamiltonian $H^{(0)}$, and want to add to its spectrum a bound state at an energy E_ϵ, while leaving all the existing bound states preserved. The following Hamiltonian in the hierarchy is constructed with the same operators as in the initial Hamiltonian (9), and with the same factorization energy E_ϵ, but in reverse order:

$$H^{(1)} = A^\dagger A + E_\epsilon \qquad (11)$$

and it has a real (physical) bound state at E_ϵ in its eigenspectrum. The normalized wavefunctions of the new Hamiltonian are given by

$$\psi_i^{(1)}(z) = \frac{1}{\sqrt{E_i^{(0)} - E_\epsilon}} A^\dagger \psi_i^{(0)}(z), \qquad i \neq \epsilon \qquad (12)$$

or, after performing the operator action

$$\psi_i^{(1)}(z) = \frac{\hbar}{\sqrt{2m^* \left(E_i^{(0)} - E_\epsilon\right)}} \frac{\mathrm{W}\left\{\psi_i^{(0)}(z), \psi_\epsilon^{(0)}(z)\right\}}{\psi_\epsilon^{(0)}(z)} \qquad (13)$$

where

$$\mathrm{W}\left\{\psi_i^{(0)}, \psi_\epsilon^{(0)}\right\} = \psi_i^{(0)}\frac{d}{dz}\psi_\epsilon^{(0)} - \psi_\epsilon^{(0)}\frac{d}{dz}\psi_i^{(0)}$$

is the Wronskian. In the case $i = \epsilon$, however, the wavefunction

$$\psi_\epsilon^{(1)}(z) = \frac{1}{\psi_\epsilon^{(0)}(z)} \qquad (14)$$

has to be normalized numerically. The potential energy corresponding to the new Hamiltonian is

$$U^{(1)}(z) = U^{(0)}(z) - \frac{\hbar^2}{m^*}\frac{d^2}{dz^2}\ln\psi_\epsilon^{(0)}(z). \qquad (15)$$

For $U^{(1)}(z)$, $\psi_\epsilon^{(1)}(z)$, and $\psi_i^{(1)}(z)$ to be free of singularities, it is necessary that $\psi_\epsilon^{(0)}(z)$ never cross zero. The function $\psi_\epsilon^{(0)}(z)$ may be written as

$$\psi_\epsilon^{(0)}(z) = \zeta(z)\left(\lambda_{\mathrm{SUSY}} + \int_{-\infty}^z \frac{1}{\zeta^2(z')}\,dz'\right) \qquad (16)$$

and if $\zeta(z)$ has no zeros, the integral $\int_{-\infty}^z 1/\zeta^2(z')\,dz'$ remains finite for any value of z. To ensure that, under this condition, $\psi_\epsilon^{(0)}(z)$ also has no zeros, the free parameter λ_{SUSY} should satisfy

$$\lambda_{\mathrm{SUSY}} \notin \left[0, -\int_{-\infty}^z \frac{1}{\zeta^2(z')}\,dz'\right]. \qquad (17)$$

By varying the parameter λ_{SUSY} in the allowed range, one gets the family of isospectral potentials

$$U^{(1)}(z, \lambda_{\mathrm{SUSY}}) = U^{(0)}(z) - \frac{\hbar^2}{m^*}\frac{d^2}{dz^2}$$
$$\cdot \ln\left[\zeta(z)\left(\lambda_{\mathrm{SUSY}} + \int_{-\infty}^z \frac{1}{\zeta^2(z')}\,dz'\right)\right] \qquad (18)$$

which all have the energy spectrum identical to that of the initial potential $U^{(0)}(z)$, with an additional real state at E_ϵ. To make the function $\zeta(z)$, which has no zeros, we write it as the linear
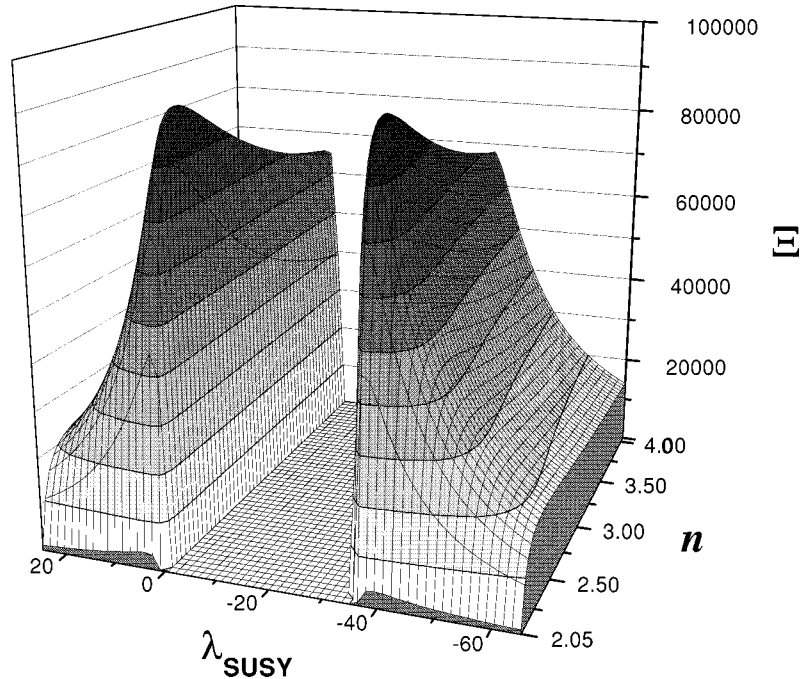
Fig. 1.   Parameter Ξ, which determines the laser gain, as it depends on parameters n (in the Pöschl–Teller potential) and λ_{SUSY} (in SUSYQM), calculated for $\Delta E_{21} = 80$ meV. The maximal value $\Xi = 99\,000$ psÅ^4 is obtained with $n^{\mathrm{opt}} = 2.35$ and $\lambda_{\mathrm{SUSY}}^{\mathrm{opt}} = -35.8$.

combination of particular solutions $\zeta(z) = \zeta_-(z) + \zeta_+(z)$ of the Schrödinger equation

$$\left(-\frac{\hbar^2}{2m^*}\frac{d^2}{dz^2} + U^{(0)}(z) \right) \zeta_\pm(z) = E_\epsilon \zeta_\pm(z) \qquad (19)$$

satisfying the boundary conditions $\zeta_-(-\infty) = 0$ and $\zeta_+(+\infty) = 0$.

III. NUMERICAL RESULTS AND DISCUSSION

In order to demonstrate the procedure for the optimization of the QW shape (i.e., the gain maximization), we choose for the initial potential the family of Pöschl–Teller potentials

$$V_{PT}(z) = -\frac{\hbar^2}{2m^*a^2}\frac{n(n+1)}{\cosh^2\left(\frac{z}{a}\right)} \qquad (20)$$

with the parameter $n \in \Re$. An advantage of this potential is that all of its eigenenergies are known analytically [27], allowing one to relate the level spacings to the potential parameters. For instance, the spacing between the lowest two states ΔE_{21} (these will be the lower and upper laser state, if this QW is to be used for such a purpose) is in this work set to 80 meV, corresponding to the laser wavelength of $\lambda \approx 15.5$ μm, so that $\Delta E_{21} + \hbar\omega_{\mathrm{LO}} = 116$ meV equals the CO$_2$ pump laser photon energy. This requires the parameters a and n to be related as $a = [\hbar^2(n-(3/2))/m^*\Delta E_{21}]^{-1/2}$, where n has to be ≥ 2 if the well is to accommodate at least two bound states (note that just two states, *not three*, suffice in this phase of design). By varying n, therefore, one finds a family of potentials, of different shapes, but with ΔE_{21} fixed.

Tuning of the QW ground state, so that it is spaced by one optical phonon energy from the lower laser state and by the pump photon energy ($\hbar\omega_p = 116$ meV) from the upper laser state, was performed by actually adding such a state at E_ϵ, using SUSYQM. Particular solutions were found for the Schrödinger equation with the potential $U^{(0)} \equiv V_{PT}(z)$ at an energy $E_\epsilon = E_1^{(0)} - \hbar\omega_{\mathrm{LO}}$ which is not its eigenenergy, as described above, and the new potential $U^{(1)}(z)$ could be further varied (asymmetrized to have $z_{\epsilon 2} \neq 0$) by varying the constant λ_{SUSY}. This procedure was repeated for the whole family of Pöschl–Teller potentials, i.e., corresponding to different values of the n parameter (with the constraint that ΔE_{21} is fixed, as noted above). Thus, the $(n, \lambda_{\mathrm{SUSY}})$ parameter space could be searched for the maximum of the product Ξ, Fig. 1.

After performing this search, we find that the parameter values $n^{\mathrm{opt}} = 2.35$ and $\lambda_{\mathrm{SUSY}}^{\mathrm{opt}} = -35.8$ provide the maximal value of $\Xi = 99\,000$ psÅ^4, and the corresponding SUSY potential is given by solid line in Fig. 2. This optimized Ξ exceeds by about 50% the value obtained in the ACQW system [19], [20]. The truly smooth optimal potential cannot be realized, however, so we have discretized it, choosing the step size of three crystalline monolayers (3×2.83 Å in AlGaAs). The profile of this step-graded QW is also given in Fig. 2. This discretization slightly changes the parameters obtained within the smooth-potential model, and next we give both sets, with the values in brackets corresponding to the discretized case. We note that, consistent with the notation used in the SUSYQM considerations, $|\epsilon\rangle$ is the ground state, introduced by the SUSYQM procedure, while $|1\rangle$ and $|2\rangle$ are the already existing lower and upper laser states. Only later on, when further manipulating the optimized potential to get profiles not directly delivered by SUSYQM, will we switch to the more conventional labeling of states with the subscripts 1, 2, and 3. Thus, the dipole matrix elements in the optimized QW amount to $z_{\epsilon 2} = 11.4(10.8)$ Å and $z_{21} = 27.8(27.9)$ Å.
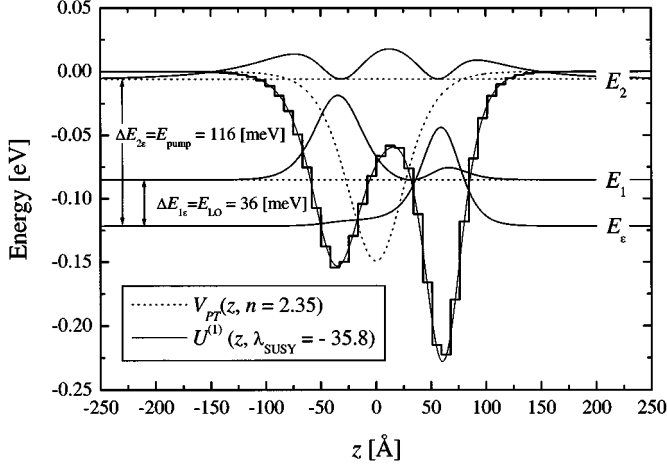
Fig. 2. SUSY-optimized QW profile $U^{(1)}(z)$ and its discretized version with three-monolayers-wide steps. The potential $U^{(1)}(z)$ is obtained by starting with symmetric Pöschel–Teller potential $V_{PT}(z)$, also depicted (dotted) with its eigenstates E_1 and E_2. These two are simultaneously the excited eigenstates of the potential $U^{(1)}(z)$, while its ground state E_c results from the SUSY mapping procedure.

TABLE I
SCATTERING RATES WITH ACOUSTIC PHONONS W_{ij}^a AND WITH POLAR
OPTICAL PHONONS W_{ij}^{po}, AT $k_{\parallel} = 0$, IN [1/PS] UNITS

	SUSY QW	Diffusion	3 × m.l.	Final
W_{21}^a	4.16×10^{-3}	4.34×10^{-3}	4.08×10^{-3}	2.84×10^{-3}
W_{31}^a	3.97×10^{-3}	4.92×10^{-3}	4.04×10^{-3}	8.64×10^{-3}
W_{32}^a	4.36×10^{-3}	4.50×10^{-3}	4.39×10^{-3}	5.17×10^{-3}
W_{21}^{po}	2.283	2.351	1.955	1.564
W_{31}^{po}	0.309	0.381	0.317	0.577
W_{32}^{po}	0.489	0.503	0.497	0.504

Carrier relaxation times were calculated using the expressions for bulk-like polar optical and acoustical phonon scattering (given in Table I), within the parabolic approximation (Section II-A), and amount to $\tau_{1\epsilon} = 0.44(0.51)$, $\tau_{2\epsilon} = 3.19(3.16)$, $\tau_{21} = 2.03(2.01)$, and $\tau_2 = 1.24(1.23)$ ps. Certainly, since the SUSYQM procedure was used, the interlevel spacings are exactly as required, i.e., $\Delta E_{2\epsilon} = 116$ and $\Delta E_{1\epsilon} = 36$ meV, with the energies of the three states individually being $E_\epsilon = -121.76(-121.57)$, $E_1 = -85.76(-85.14)$, and $E_2 = -5.76(-5.99)$ meV. The modal gain which could be obtained in such an optimized structure at $T = 77$ K exceeds $G_m = 1.84 \times 10^{-3}$ ($g = 980$ cm^{-1}) for pump powers ≥ 500 kW·cm^{-2}.

An alternative route to approximate realization of the optimal smooth potential is to start with a structure which has a small number of layers and use the interdiffusion process. In the course of post-growth heat treatment of (typically) initially stepwise-constant QW structures, the constituent materials diffuse toward smoothed profiles, hence changing the potential, wavefunctions, and energies. This technique has been successfully employed for tuning the wavelength of AlGaAs-based intersubband infrared photodetectors [28], or for tuning the polarization properties of interband lasers based on a more complex, 4-atomic-species system [29]. Here, we demonstrate that it is possible to use this technique to generate QW profiles resembling those derived as optimal for the laser.

Consider a structure made of N layers of Al$_x$Ga$_{1-x}$As with an Al mole fraction in each layer x_j (constant within a layer), embedded in bulk of the composition x_0 on the left and x_{N+1} on the right of the multilayer stack. In a specified coordinate system, the left boundary of jth layer is denoted as z_{j-1}, and the right boundary as z_j (i.e., the width of jth layer is $z_j - z_{j-1}$). Starting with this stepwise-constant profile, due to the interdiffusion by thermal annealing at constant temperature, the profile will change in time according to [28]–[30]

$$x(z, t) = \sum_{j=1}^{N} \frac{x_j}{2} \left[\text{Erf}\left(\frac{z - z_{j-1}}{L_d} \right) - \text{Erf}\left(\frac{z - z_j}{L_d} \right) \right]$$
$$+ \frac{x_0}{2} \left[1 - \text{Erf}\left(\frac{z - z_0}{L_d} \right) \right]$$
$$+ \frac{x_{N+1}}{2} \left[1 + \text{Erf}\left(\frac{z - z_N}{L_d} \right) \right] \tag{21}$$

where
$L_d = 2\sqrt{Dt}$—diffusion length;
D diffusion coefficient, which depends on the annealing temperature (this dependence is given in [30] for the AlGaAs system);
t annealing time.
Note that the influence of temperature (via the coefficient D) and time is, in the case of the AlGaAs system, grouped into a single parameter L_d, but in 4-component systems, these would come in independently. The question is then, given the desired profile $x_{\text{target}}(z)$, how can one design the initial structure, i.e., choose the widths and compositions of inner layers, so that after the interdiffusion (specified by the additional free parameter L_d) the resulting profile $x(z, t)$ is as close as possible to $x_{\text{target}}(z)$. For an N-layer structure, there are thus $2N+1$ free parameters, while the bulk compositions on the left and right are actually fixed by $x_{\text{target}}(z)$ itself. For whatever finite N, it is generally impossible to get the full coincidence of the two profiles, but good agreements may be obtained by fitting.

We have attempted to design a good initial structure with just $N = 3$ inner layers which, after interdiffusion, will reproduce the optimal potential to a good accuracy. Thus, we found that the structure Al$_{0.093}$Ga$_{0.907}$As (53.705 Å $= 19$ m.l.)–Al$_{0.22}$Ga$_{0.78}$As (50.879 Å $= 18$ m.l.)–GaAs (42.399 Å $= 15$ m.l.)—embedded in Al$_{0.28}$Ga$_{0.72}$As outer barriers bulk (Fig. 3), after the interdiffusion characterized by $1/L_d = 0.0525$ Å^{-1}, delivers the profile maximally similar to the target, SUSYQM-optimized profile, both being also given in Fig. 3. This was the best that could be obtained from the three-layer initial structures. Certainly, even better fits could be obtained with larger N, but we wanted to keep the initially grown structure as simple as possible. Yet, checking various relevant quantities corresponding to the interdiffused profile, shows that is quite good: $\Delta E_{31} = 114.7$ and $\Delta E_{21} = 36.1$
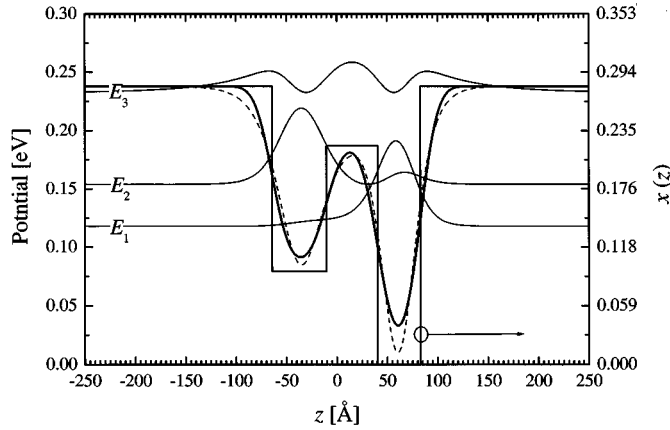
Fig. 3.   Profile of the initial stepwise-constant three-layer structure used for interdiffusion, and the profile generated by it (solid line). The target, SUSYQM-optimized potential is also displayed (dashed line).
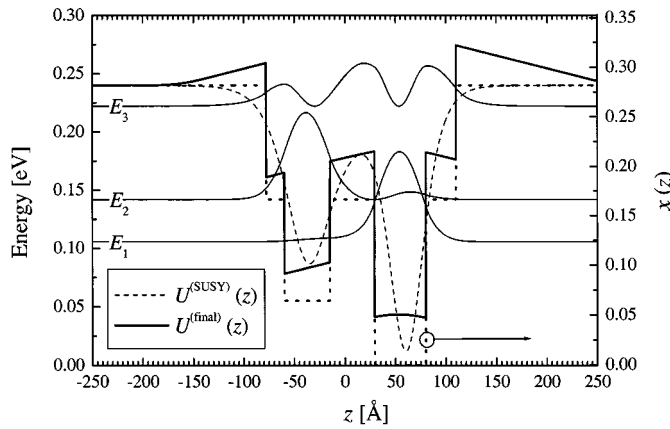

Fig. 4.   The final coarse-discretized and the self-consistent potential. Dotted line: Al mole fraction (grading) profile in the $Al_x Ga_{1-x} As$ alloy, to be read on the right vertical axis.

meV, $z_{13} = 11.5$ and $z_{23} = 28.4$ Å, $\tau_{21} = 0.42$, $\tau_{31} = 2.59$, $\tau_{32} = 1.97$, and $\tau_3 = 1.12$ ps. That is, starting with the simple three-layer structure and performing the interdiffusion will deliver the gain parameter $\Xi = 94\,000$ ps·Å^4 rather close to the value corresponding to the SUSYQM-optimized profile. The modal gain at $T = 77$ K in it exceeds $G_m = 1.79 \times 10^{-3}$ ($g = 940$ cm^{-1}) for the pump power ≥ 500 kW·cm^{-2}.

Returning to the discretization of the smooth optimal potential, and not relying on the interdiffusion, various coarse discretizations may be employed which will make the structure more or less easily realizable. Yet, the states energies will then become more remote from the designed values, and some fine tuning of layers widths and potential heights may be needed. At this point, however, one may take account of various, relatively small but not negligible, effects that would be extremely difficult to handle by the SUSYQM directly. Here, we have taken into account the position-dependent effective mass, and the self-consistent potential. The latter is calculated by iteratively solving the Schrödinger and Poisson equations [31]. Thus, we have designed a five-layer structure: $Al_{0.17}Ga_{0.83}As$ (18 Å)–$Al_{0.06}Ga_{0.94}As$ (45 Å)–$Al_{0.17}Ga_{0.83}As$ (44 Å)–GaAs (51 Å)–$Al_{0.17}Ga_{0.83}As$ (30 Å), embedded in $Al_{0.28}Ga_{0.72}As$ outer
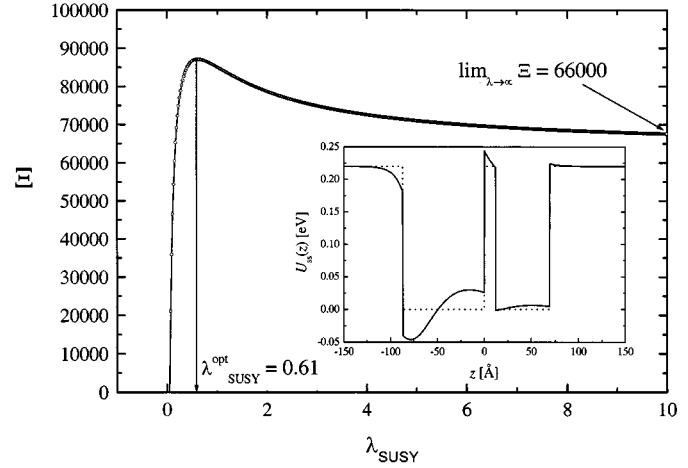

Fig. 5.   Gain parameter Ξ as it depends on the transform parameter λ_{SUSY} in the fully isospectral SUSYQM transform applied to the stepwise-constant ACQW (the no-transform limit corresponds to taking $\lambda_{SUSY} \to \infty$). Inset: the optimal profile, giving the maximal value of Ξ.

barrier bulk, Fig. 4. Modulation doping to $n_s = 3 \times 10^{11}$ cm^{-1} is assumed, the doped region being 50 Å wide and 60 Å away from the QW boundary. The energy spacings in this structure (at $k_{\parallel} = 0$) amount to $\Delta E_{21} = 36.25$ and $\Delta E_{32} = 80.26$ meV, and the Fermi level E_F is 9.1 meV above the ground state. At $T = 77$ K the ratio of carrier densities on the ground and the lower laser state is $n_1/n_2 \approx 10^2$. The dipole matrix elements in this structure are calculated to be $z_{13} = 14.9$ and $z_{23} = 24.9$ Å, the relaxation times are $\tau_{21} = 0.63$, $\tau_{31} = 1.71$, $\tau_{32} = 1.96$, and $\tau_3 = 0.91$ ps, and the gain parameter is $\Xi = 86\,000$ psÅ^4. The modal gain would, thus, exceed $G_m = 1.51 \times 10^{-3}$ ($g = 800$ cm^{-1}) at the pump intensity ≥ 500 kWcm^{-2} and $T = 77$ K. The gain saturation starts at pump intensities ≥ 10 MWcm^{-2}, the saturated modal gain being $G_m \simeq 2.82 \times 10^{-3}$. By further variation of the above system, i.e., by reducing the spacing between the two wells and, hence, obtaining a stronger coupling of the states $|1\rangle$ and $|2\rangle$, one can achieve even smaller $\tau_{21} \simeq 0.4$ ps, for which the saturated gain would be as large as $G_m \simeq 4.70 \times 10^{-3}$. We should also note that, in an ACQW structure, optimized according to the gain/loss criterium (see [19] and [20] for details), one finds $z_{13} = 15$ Å, $z_{23} = 25$ Å, $\tau_{21} = 0.5$ ps, $\tau_{31} = 1.2$ ps, and $\tau_{32} = 1.5$ ps; hence, $G_m = 1.20 \times 10^{-3}$ (in this structure, the transition $|2\rangle \mapsto |1\rangle$ was set to 39 meV in order to decrease the thermal population of the lower laser state and improve the system dynamics). Therefore, this structure has about a 26% smaller modal gain G_m than the final structure presented in this work.

As for the comparison of the performance of various complex structures described in this work, against that of the conventional three-layer stepwise-constant profile QW, it is relatively straightforward to show that the latter does not have the optimal shape for the optically pumped laser. Here we start with an ACQW (with $\Delta E_{21} = 36$ meV and $\Delta E_{31} = 116$ meV) and subject it to a fully isospectral SUSYQM transform, as in [32], rather than to the state-adding transform used in this work. By varying the transform parameter λ_{SUSY}, we find the optimal value $\lambda_{SUSY}^{opt} = 0.61$, which gives the value of the product $\Xi = 88\,000$ psÅ^4, i.e., about 33% better result than
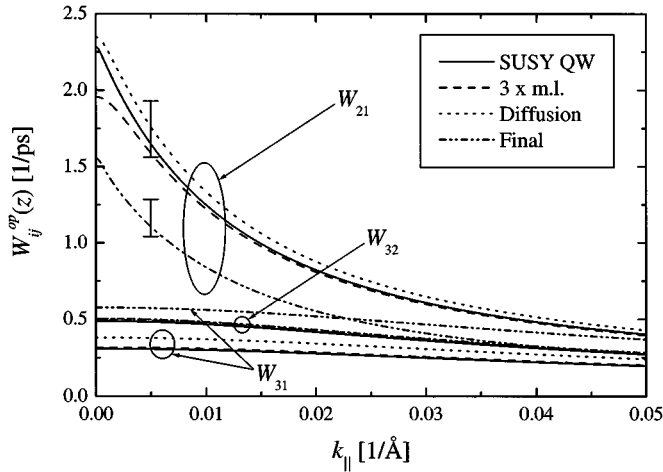
Fig. 6. Scattering rates W_{ij}^{po} versus $k_{\parallel}$ dependence, calculated for the SUSY optimized potential (solid line), the 3-monolayer-width discretized structure (dashed), the interdiffused potential (dotted), and for the final potential $U^{(\text{final})}(z)$ (dashed-dotted). The error bars indicate the uncertainty of W_{ij}^{po} due to the spread of reported values of material parameters. The error bar boundaries are approximately 16.5% above/5.5% below the stated values of W_{ij}^{po}, indicating these are reasonable estimates. The displayed error bars apply for any $k_{\parallel}$, because they originate from the $k_{\parallel}$-independent term in (6).

was obtained in the initial ACQW in which $\Xi = 66\,000$ psÅ^4 (Fig. 5). In terms of gain obtainable at the same pump power (500 kWcm^{-2}) and carrier density, the SUSY optimized well has $G_m \simeq 1.73 \times 10^{-3}$ ($g \simeq 1100$ cm^{-1}), i.e., 30% more than $G_m \simeq 1.33 \times 10^{-3}$ ($g \simeq 850$ cm^{-1}) in the initial QW. Yet, this profile, displayed in the inset of Fig. 5 is clearly very difficult to realize. It should be noted that the gain values stated in this paragraph are somewhat overestimated because the small constant effective mass $m^* = 0.0665m_0$, corresponding to GaAs, was used in the calculation, which is good enough for the purpose of comparison (for other step graded structures in this paper we used the real, Al mole fraction-dependent electron effective mass).

The electron scattering rates depend on the in-plane wavevector $k_{\parallel}$, though this is significant mostly for the transition between the lowest two states, spaced by the optical phonon energy (cf. Fig. 6). Because of low operating temperatures, we have used here the values corresponding to $k_{\parallel} = 0$ in gain calculations. At high pump intensities, as was shown in [16]–[18], considerable electron heating may occur (with different electron temperatures in each subband). Under such conditions, or simply at higher temperatures or larger doping densities, when a considerable fraction of the total carrier density also resides in states with larger $k_{\parallel}$, it may be necessary to use the appropriate averages of the scattering rates in Fig. 6. It is then that the fully self-consistent optimization, specific to the chosen carrier density, should be performed. In this work, however, we aimed at optimizing the laser profile for the case of a pump not too strong when these effects could be neglected.

At the end of this section, we will briefly discuss the confidence limits of the obtained results, in view of the fact that there is a bit of a spread of values of various material parameters in the literature, e.g., [26], [33]–[35], and a considerably larger spread of the values of the transition linewidth Γ, e.g., [17], [35], [24].

A brief analysis of the gain expression, accounting for the actual spread of various parameters, indicates that the uncertainty of the absolute value of gain is mostly determined by the uncertainty of $\{\epsilon_p/\hbar\omega_{\text{LO}}[n(\omega_{\text{LO}}) + 1]\} \cdot [1/(\tilde{n}\Gamma)^2]$. The first term comes in via the relaxation rate W_{ij}^{po}, and results in error bars given in Fig. 6, so the results we stated above are safely inside the uncertainty window. Certainly, these considerations are relevant for the absolute value of gain, not for relative comparison of different designs. In reality, however, the value of Γ appears to be much more uncertain, strongly depending on the structure quality. The value used here (and also in [17], [24], for similar type of structures) appears to be a quite conservative estimate, because smaller values (1–2 meV) are sometimes reported, e.g., [35], and these would lead to an increase of gain by more than an order of magnitude, i.e., by a factor of 18; this is because individual cross sections σ_{ij} would then each enlarge more than fourfold. An uncertainty as large as that is the reason that the parameter Ξ (itself not containing Γ) is a reasonable descriptor of the QW usefulness for laser, and was here used as the optimization target. Finally, it is also interesting to note the resemblance of the potential profiles derived here to the refractive index profiles in W-core fibers, e.g., [36], though QWs are one-dimensional, while fibers have circular symmetry—the low potential (high refractive index) portions accumulate (guide) the major part of the wavefunction (light field).

IV. CONCLUSION

A systematic procedure was proposed for QW profile optimization to get maximal gain in an optically pumped intersubband QW laser. The procedure is based on SUSYQM, used to add a bound state below the spectral range of the initial potential, and also to enable shape variation (and asymmetrization) of the new potential. The transform parameter (and possibly additional parameters, if existing in the initial potential) is then varied to find the value(s) which maximize the target function. Since the obtained optimized potential is continuously varying, it remains to discretize it into a stepwise-constant form suitable for realization. This is done in the average-over-the-step-size fashion once the step size has been decided. Final minor corrections are made, if needed because of discretization, or in order to include other effects, like the self-consistent potential. The use of this method was demonstrated on the optimized design of the AlGaAs-based intersubband laser with the predicted results well exceeding the best values published in the literature.

REFERENCES

[1] R. F. Kazarinov and R. A. Suris, "Possibility of the amplification electromagnetic waves in a semiconductor with superlattice," *Sov. Phys. Semicond.*, vol. 5, pp. 707–711, 1971.

[2] J. Faist, F. Capasso, D. L. Sivco, C. Sirtori, A. L. Hutchinson, and A. Y. Cho, "Quantum cascade laser," *Science*, vol. 264, pp. 553–556, 1994.

[3] J. Faist, F. Capasso, D. L. Sivco, C. Sirtori, J. N. Baillargeon, A. L. Hutchinson, S. N. G. Chu, and A. Y. Cho, "High power mid-infrared ($\lambda \sim 5\mu$m) quantum cascade laser operating above room temperature," *Appl. Phys. Lett.*, vol. 68, pp. 3680–3682, 1996.

[4] C. Sirtori, J. Faist, F. Capasso, D. L. Sivco, A. L. Hutchinson, and A. Y. Cho, "Long wavelength infrared ($\lambda \sim 11\mu$m) quantum cascade lasers," *Appl. Phys. Lett.*, vol. 69, pp. 2810–2812, 1996.

[5] C. Sirtori, P. Kruck, S. Barbieri, P. Collot, J. Nagle, M. Beck, J. Faist, and U. Oesterle, "GaAs/AlGaAs quantum cascade lasers," *Appl. Phys. Lett.*, vol. 73, pp. 3486–3488, 1998.

[6] M. Razeghi, D. Wu, B. Lane, A. Rybaltowski, A. Stein, J. Diaz, and H. Yi, "Recent achievement in MIR high power injection laser diodes ($\lambda = 3$ to 5μm)," *LEOS Newsletter*, vol. 13, pp. 7–10, 1999.

[7] I. Vurgaftman, J. R. Meyer, F. H. Julien, and L. H. Ram-Mohan, "Design and simulation of low threshold antimonide intersubband lasers," *Appl. Phys. Lett.*, vol. 73, pp. 711–713, 1998.

[8] G. Sun, Y. Lu, and J. B. Khurgin, "Valence intersubband lasers with inverted light-hole effective mass," *Appl. Phys. Lett.*, vol. 72, pp. 1481–1483, 1998.

[9] L. Friedman, R. Soref, and G. Sun, "Silicon-based interminiband infrared laser," *J. Appl. Phys.*, vol. 83, pp. 3480–3485, 1998.

[10] G. Sun and J. Khurgin, "Optically pumped four-level infrared laser based on intersubband transitions in multiple quantum wells: Feasibility study," *IEEE J. Quantum Electron.*, vol. 29, pp. 1104–1111, 1993.

[11] O. Gauthier-Lafaye, F. H. Julien, S. Cabaret, J.-M. Lourtioz, G. Strasser, E. Gornik, M. Helm, and P. Bois, "High-power GaAs/AlGaAs quantum fountain unipolar laser emitting at 14.5 μm with 2.5% tunability," *Appl. Phys. Lett.*, vol. 74, pp. 1537–1539, 1999.

[12] J. B. Khurgin, G. Sun, L. R. Friedman, and R. A. Soref, "Comparative analysis of optically pumped intersubband lasers and intersubband Raman oscillators," *J. Appl. Phys.*, vol. 78, pp. 7398–7400, 1995.

[13] G. Sun, J. B. Khurgin, L. Friedman, and R. A. Soref, "Tunable intersubband Raman laser in GaAs/AlGaAs multiple quantum wells," *J. Opt. Soc. Amer. B*, vol. 15, pp. 648–651, 1998.

[14] V. Berger, "Three-level laser based on intersubband transitions in asymmetric quantum wells: A theoretical study," *Semicond. Sci. Technol.*, vol. 9, pp. 1493–1499, 1994.

[15] F. H. Julien, A. Saar, J. Wang, and J.-P. Leburton, "Optically pumped intersub-band emission in quantum wells," *Electron. Lett.*, vol. 31, pp. 838–839, 1995.

[16] J. Wang, J.-P. Leburton, F. H. Julien, and A. Saar, "Design and performance optimization of optically-pumped mid-infrared intersubband semiconductor lasers," *IEEE Photon. Technol. Lett.*, vol. 8, pp. 1001–1003, 1996.

[17] J. Wang, J.-P. Leburton, Z. Moussa, F. H. Julien, and A. Saar, "Simulation of optically pumped mid-infrared intersubband semiconductor laser structures," *J. Appl. Phys.*, vol. 80, pp. 1970–1978, 1996.

[18] F. H. Julien and J.-P. Leburton, "Long wavelength infrared emitters based on quantum well and superlattices," in *Optoelectronics Properties of Semiconductors and Superlattices*, M. Helm, Ed. New York: Gordon and Breach, 2000, vol. 6, pp. 89–134.

[19] O. Gauthier-Lafaye, P. Boucaud, F. H. Julien, S. Sauvage, S. Cabaret, J.-M. Lourtioz, V. Thierry-Mieg, and R. Planel, "Long-wavelength ($\sim 15.5\mu$m) unipolar semiconductor laser in GaAs quantum wells," *Appl. Phys. Lett.*, vol. 71, pp. 3619–3621, 1997.

[20] O. Gauthier-Lafaye, S. Sauvage, P. Boucaud, F. H. Julien, F. Glotin, R. Prazeres, J.-M. Ortega, V. Thierry-Mieg, and R. Planel, "Investigation of mid-infrared intersubband stimulated gain under optical pumping in GaAs/AlGaAs quantum wells," *J. Appl. Phys.*, vol. 83, pp. 2920–2926, 1998.

[21] C. V. Sukumar, "Supersymmetrc quantum mechanics in one-dimensional systems," *J. Phys. A*, vol. 18, pp. 2917–2936, 1985.

[22] F. Cooper, A. Khare, and U. Sukhatme, "Supersymmetry and quantum mechanics," *Phys. Rep.*, vol. 251, pp. 267–385, 1995.

[23] P. Blood, "On the dimensionality of optical absorption, gain, and recombination in quantum-confined structures," *IEEE J. Quantum Electron.*, vol. 36, pp. 354–362, 2000.

[24] F. H. Julien, Z. Moussa, P. Boucaud, Y. Lavon, A. Saar, J. Wang, J.-P. Leburton, V. Berger, J. Nagle, and R. Planel, "Intersubband mid-infrared emission in optically pumped quantum wells," *Superlatt. Microstruct.*, vol. 19, pp. 69–79, 1996.

[25] B. K. Ridley, "The electron–phonon interaction in quasitwo-dimensional semiconductor quantum well structures," *J. Phys. C: Solid State Phys.*, vol. 15, pp. 5899–5917, 1982.

[26] S. Adachi, "GaAs, AlAs, and Al$_x$Ga$_{1-x}$As: Material parameters for use in research and device applications," *J. Appl. Phys.*, vol. 58, pp. R1–R29, 1985.

[27] S. Flügge, *Practical Quantum Mechanics*. Berlin, Germany: Springer-Verlag, 1974.

[28] X. Liu, N. Li, X. Chen, W. Lu, W. Xu, X. Z. Yuan, N. Li, S. C. Shen, S. Yuan, H. H. Tan, and C. Jagadish, "Wavelength tuning of GaAs/AlGaAs quantum-well infrared photodetectors by thermal interdiffusion," *Jpn. J. Appl. Phys.*, vol. 38, pp. 5044–5045, 1999.

[29] W. C. H. Choy, "Tailoring light and heavy holes of GaAsP–AlGaAs quantum wells by using interdiffusion for polarization-independent amplifier applications," *IEEE J. Quantum Electron.*, vol. 36, pp. 164–171, Feb. 2000.

[30] T. E. Schlesinger and T. Kuech, "Determination of the interdiffusion of Al and Ga in undoped (Al,Ga)As/GaAs quantum wells," *Appl. Phys. Lett.*, vol. 49, pp. 519–521, 1986.

[31] Z. Ikonić, V. Milanović, and D. Tjapkin, "Resonant second harmonic generation by a semiconductor quantum well in electric field," *IEEE J. Quantum Electron.*, vol. 25, pp. 54–60, Jan. 1989.

[32] S. Tomić, V. Milanović, and Z. Ikonić, "Optimization of intersubband resonant second-order susceptibility in asymmetric graded Al$_x$Ga$_{1-x}$As quantum wells using the supersymmetric quantum mehanics," *Phys. Rev. B*, vol. 56, pp. 1033–1036, 1997.

[33] O. Madelung, *Data in Science Technology. Semiconductors: Group IV Elements and III–V Compounds*. Berlin, Germany: Springer-Verlag, 1991.

[34] *INSPEC: Properties of Galium Arsenide*, 3rd ed., M. R. Brozel and G. E. Stillman, Eds., 1996.

[35] E. H. Li, "Material parameters of InGaAsP and InAlGaAs systems for use in quantum well structures at low and room temperatures," *Physica E*, vol. 5, pp. 215–273, 2000.

[36] M.-S. Wu, M.-H. Lee, and W.-H. Tsai, "Variational analysis of single-mode graded-core W-fibers," *IEEE J. Lightwave Technol.*, vol. 14, pp. 121–125, 1996.

Stanko Tomić was born in Belgrade, Yugoslavia, in 1967. He received the B.Sc., M.Sc., and Ph.D. degrees in electrical engineering from the University of Belgrade, Belgrade, Yugoslavia, in 1993, 1996, and 1998, respectively.

In 1993, he joined VINČA Institute of Nuclear Sciences, Belgrade, Yugoslavia, where he has been engaged in research and development of TESLA accelerator installation. Currently, he is a Research Fellow in the Optoelectronics Devices and Materials Group at the University of Surrey, Guildford, U.K. His research interests include QW lasers, nonlinear optical properties of QWs, and accelerator physics.

Vitomir Milanović was born in Svetozarevo, Yugoslavia, in 1947. He received the B.Sc., M.Sc., and Ph.D. degrees in electrical engineering from University of Belgrade, Belgrade, Yugoslavia, in 1971, 1977, and 1983, respectively.

He is currently a Full Professor with the Faculty of Electrical Engineering, University of Belgrade, Belgrade, Yugoslavia. His research interests include the electronic structure and optical properties of QWs and superlattices.

Zoran Ikonić was born in Belgrade, Yugoslavia, in 1956. He received the B.Sc., M.Sc., and Ph.D. degrees in electrical engineering from University of Belgrade, Belgrade, Yugoslavia, in 1980, 1984, and 1987, respectively.

He is a Full Professor at the Faculty of Electrical Engineering, University of Belgrade, currently on leave from the University of Leeds, Leeds, U.K. His research interests include band-structure calculations and nonlinear optics of QWs and superlattices.